

The Effect of Layer Thickness and Orientation of 3D Printed Workpieces, on The Micro- and Macrogeometric properties of Turned Parts

Gábor Kónya^{1*}, Péter Ficzer²

¹Department of Innovative Vehicles and Materials, GAMF Faculty of Engineering and Computer Science, John von Neumann University, Izsáki út 10, H-6000 Kecskemét, Hungary; konya.gabor@nje.hu

²Department of Railway Vehicles and Vehicle System Analysis, Faculty of Transportation Engineering and Vehicle Engineering, Budapest University of Technology and Economics, Műegyetem rkp. 3, H-1111 Budapest, Hungary; ficzere.peter@kjk.bme.hu

Abstract: 3D printing technologies have developed significantly over the last 30 years, having a major impact on all segments of today's industry. Additive Manufacturing (AM) offers the possibility to produce both prototype and finished parts, reducing product development time and costs while producing higher quality results. However, producing high precision and quality surfaces, such as threads, is still difficult with 3D printing technologies. To eliminate these problems, there are already machines that combine some form of the 3D printing process and of subtractive manufacturing technology. In this type of production, extra material is always left on the surface of the workpiece during the printing process, and functional surfaces are created by removing this extra material. In this scientific study, the authors have dealt with the effect of layer thickness and orientation of the 3D printed workpiece, for the micro- and macro-geometric properties, on the printed and the machined (turned) parts. The authors measured the surface roughness, the deviation from nominal size and determined the cylindricity, after printing and machining. During turning, the effects of printing orientation and chip formation process were investigated. The aim was to investigate the effect of the orientation and layer thickness of the printed objects, on the quality and cylindricity of the final turned parts.

Keywords: 3D printing; PLA; turning; cylindricity, surface roughness

1 Introduction

3D printing has revolutionized the automotive industry in several ways. By allowing for rapid prototyping, companies can quickly test and refine their designs, which results in faster time-to-market and reduced costs [1]. Additionally,

the ability to produce high-quality parts with complex geometries and internal structures has led to increased design freedom, enabling the creation of lighter and more efficient components. This, in turn, has made it possible to develop new vehicles that are lighter, more efficient, and have improved performance characteristics. Overall, the use of 3D printing technology in the automotive industry has resulted in a more flexible, efficient, and cost-effective manufacturing process [2] [3].

Utilizing Additive Manufacturing (AM), also known as 3D printing, which produces parts layer by layer based on models created with Computer Aided Design (CAD), it is possible to design geometries that would be difficult or even impossible to realize using traditional manufacturing methods [4]. These technologies allow greater design freedom, such as generative design, which allows conventional parts to be replaced by lighter parts with identical or improved strength characteristics. In addition, the option to print parts from multiple materials has opened up new avenues for innovation, allowing manufacturers to produce composite parts [5] that offer improved performance and durability [6] [7]. In conclusion, 3D printing has had a profound impact on the automotive industry, enabling the development of lighter, safer, and more environmentally friendly vehicles that offer improved performance and efficiency [8].

There are numerous papers comparing 3D printing processes, but the most comprehensive study was carried out by Hanon *et al.* According to this study, FDM (Fused Deposition Modelling) was found to be the most favorable 3D printing process based on several factors, including accuracy, printable size, post-processing, number of raw materials, machine size, and price of the machine [9]. While FDM may not have the highest accuracy compared to other 3D printing processes, it can still be an excellent choice for some applications. For example, if precise and aesthetically outstanding finishes are not a requirement, and functional surfaces can be post-machined, FDM can provide an affordable and efficient solution. Based on the findings of Hanon's paper, FDM 3D printing technology was selected for this study because it is relatively cheap compared to other 3D printing processes and has a wide range of available materials, therefore, it is widely used by companies [10].

In FDM 3D printing, the thermoplastic polymer filament is melted inside the extruder and then extruded through a nozzle onto the build platform. The extruder head moves along the "x-y" axes to create a cross-sectional layer of the model, and the platform is lowered in the "z" direction after each layer is completed. This process is repeated until the entire model is built up layer by layer, as shown in Fig. 1 [11] [12].

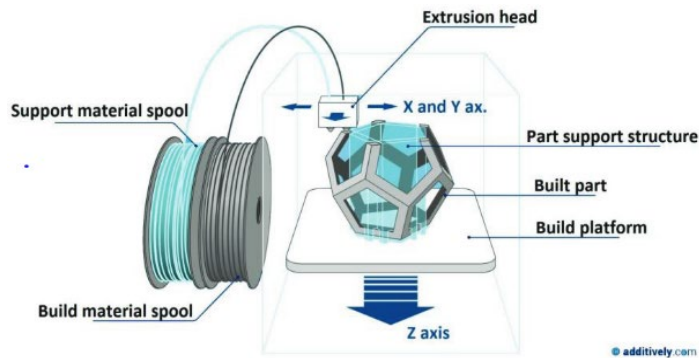


Figure 1

Printed method of FDM 3D printing

However, 3D printing processes are unable to print with the accuracy and surface quality that is a necessity in cases where high precision is required, such as a sealing surface. Even options that can be modified during pre-processing are not sufficient to improve these factors [13]. This is also typical for plastic and metallic parts, which often require post-machining [14]. Research work on PLA machining cannot be found in the literature. However, other engineering plastics, such as ABS or POM-C were turned [15] [16]. In both cases, the authors found that higher cutting speed and medium depth of cut are the more important when turning these materials.

This paper investigates the effects of layer thickness and orientation of the parts on the surface roughness, cylindricity and turning process. The aim is to determine what layer thickness and orientation is appropriate for printing products whose functional surfaces will be finished by turning.

2 Methodology

2.1 3D Printer and Printing Technology

The Prusa i3 is a popular and widely used 3D printer known for its reliability, affordability, and ease of use. Printing with PLA (Polylactic Acid) is a common choice for many 3D printing applications due to its good dimensional stability, low shrinkage, and ease of printing. PLA is a thermoplastic that is derived from renewable resources and is known for producing high-quality prints with a smooth surface finish [17]. The properties of PLA can vary depending on the specific manufacturer, but the ranges listed in Table 1 should give a good idea of the material's general characteristics.

Table 1
Property ranges for PLA materials [18] [19]

Properties	PLA
Tensile strength (MPa)	15.5-72.2
Tensile modulus (GPa)	2.020-3.550
Elongation at break (%)	0.5-9.2
Flexural strength (MPa)	52-115.1
Flexural modulus (GPa)	2.392-4.930
Printing temperature (°C)	190-220
Printing speed (mm/s)	40-90

By printing a total of 8 cylindrical test pieces with different orientations, you can gain a better understanding of the effects of orientation on the mechanical properties of the printed parts, therefore 4-4 Ø20X50 mm workpieces were printed with 0.05, 0.1, 0.2 and 0.4 mm layer thickness, as shown in Fig. 2.

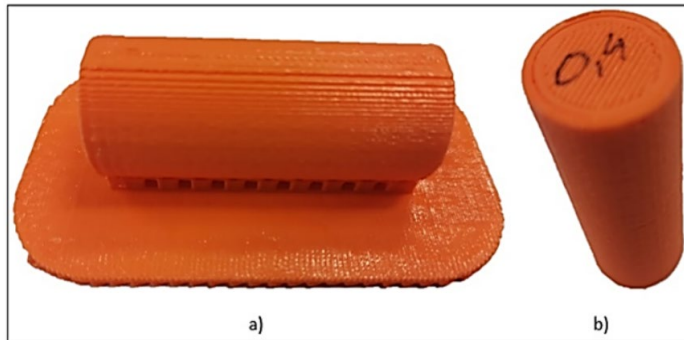


Figure 2
Printed workpieces: a) horizontal, b) vertical

The use of a CAD software like Solid Edge to model the cylinder and export an STL file is a common practice in 3D printing. The STL file format is widely used in 3D printing as it describes a 3D object as a series of triangles that make up the surface of the object. The angle subtended by the planes and tolerance specified during the export process can affect the overall accuracy and quality of the printed part. During the exporting, the angle subtended by the planes was 3° and the tolerance was 0.05 mm. Choosing the right structure is very important as it can influence not only the geometric dimensions but also the material properties [20]. Printing was done with a 30% density gyroid type fill, because it is known for its good mechanical properties and is often used in high-strength applications. [21].

When printing parts in a horizontal orientation, it is often necessary to use support material to ensure the printed part has adequate stability during the printing process. The support material helps to hold up the overhanging or cantilevered portions of the part, preventing them from collapsing or warping during printing.

The design of the support material is a crucial factor, as it can affect the overall quality and accuracy of the printed part. Therefore, at places with up to 40° inclination support material was utilized. This is shown with the gyroid infill in Fig. 3.

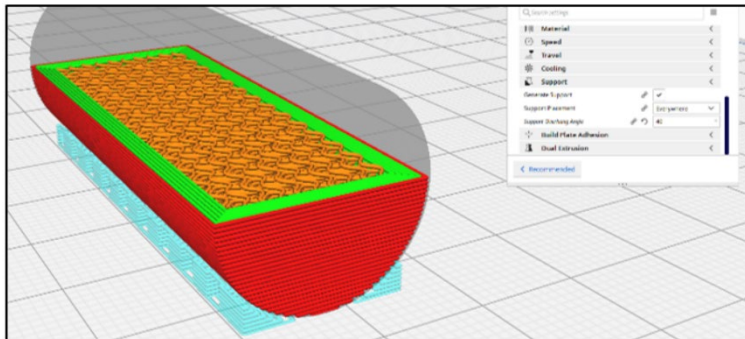


Figure 3

Production planning for the horizontally oriented workpieces

Note: horizontal orientation, 0.4 mm layer thickness

In order to carry out the turning experiments, the number of top and bottom layers of horizontal oriented pieces has been increased, otherwise the infill part would start earlier and the workpiece would not conform during machining. This can also cause errors, as the concentricity of the walls during printing can only be ensured layer by layer. For the unsupported parts, where the wall is supposed to be sufficiently steep, it was necessary to use active cooling because without it the layers became misaligned, as shown in Fig. 4.

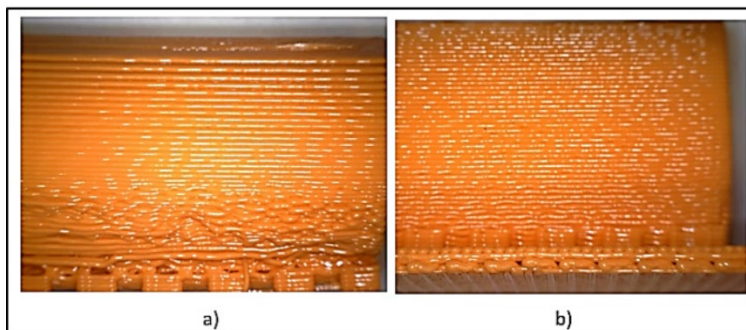


Figure 4

Printed part a) without active cooling, b) with active cooling

Note: 0.4 mm layer thickness, horizontal orientation

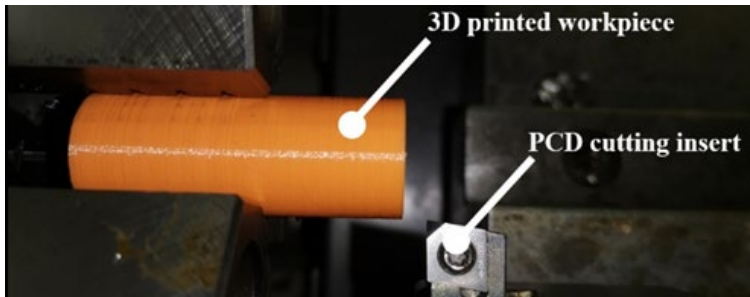
The printing parameters are listed in Table 2.

Table 2
Printing parameters

Properties	PLA
Layer thickness (mm)	0.05; 0.1; 0.2; 0.4
Wall thickness (mm)	2.5
Filling density (%)	30
Printing temperature (°C)	215
Printing speed (mm/s)	40
Fill printing speed (mm/s)	40
Active cooling	-

2.2 Cutting Parameters

After the surface roughness and cylindricity measurement of the 3D printed parts, each part was turned with the following parameters: cutting speed was $v_c = 100$ m/min, feed rate was $v_f = 0.3$ mm/rev. and the depth of cut was varied because the aim was to achieve a workpiece diameter of 18 mm in order to make the dimensional accuracy comparable. The cutting experiments were carried out on the NCT Euroturn 12 CNC lathe. A PCD (polycrystalline diamond) insert was used for the machining, as illustrated in Fig. 5.

Figure 5
Experimental setup for turning

2.3 Surface Roughness Measurement

Measuring the surface roughness of the printed parts is an important step in evaluating the quality of the printed parts. A Mitutoyo Formtracer SV-C3100 tactile roughness tester was used for measuring the surface roughness of the workpieces according to MSZ EN IS 4287:2002 and the results were evaluated in Microsoft Excel. This information can help to determine which parameters have a notable influence on the average surface roughness (R_a).

2.4 Cylindricity Measurement

For cylindricity, each point on the real cylindrical surface must be located between two coaxial cylindrical surfaces with a radius difference of the specified tolerance [22], as shown in Fig. 6. Cylindricity was measured in a prism using a Mitutoyo 543-270B dial indicator with an accuracy of 0.01 mm, assessing the dimensional deviation from the nominal size. The Roundness Measurement System could not be used because the dimensional deviation was too large. The measurement was taken from the end of the workpiece in three planes at 5, 10 and 15 mm. Four measurements were taken in each plane at 0°, 90°, 180° and 270°, as illustrated in Fig. 7. and the results were evaluated in Microsoft EXCEL.

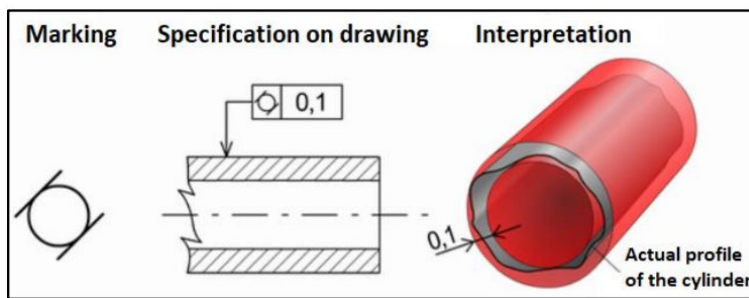


Figure 6

Interpretation of cylindricity, adapted from [22]

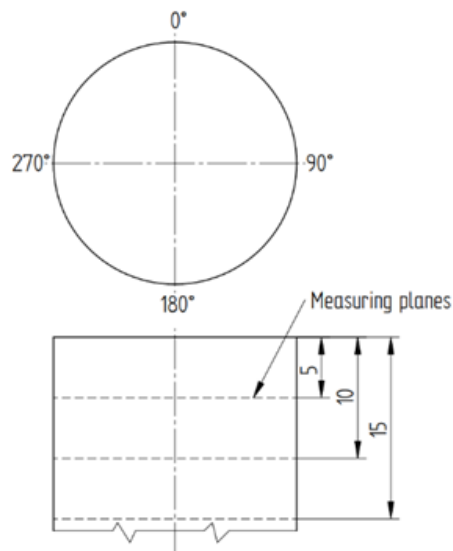


Figure 7

Principle of measurement

3 Results

3.1 Results of Surface Roughness Measurement

The roughness profiles measured after printing and turning for each layer thicknesses and orientations are shown in Fig. 8-15.

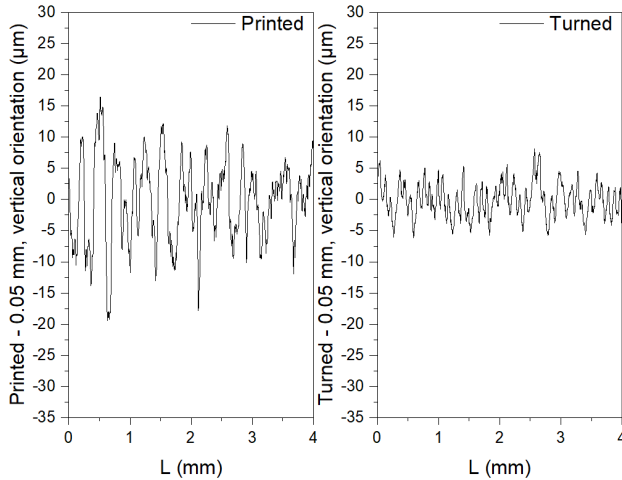


Figure 8
Roughness profiles after printing and turning

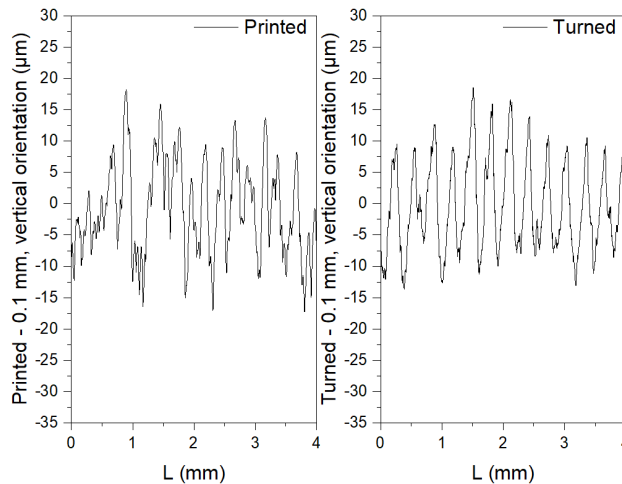


Figure 9
Roughness profiles after printing and turning

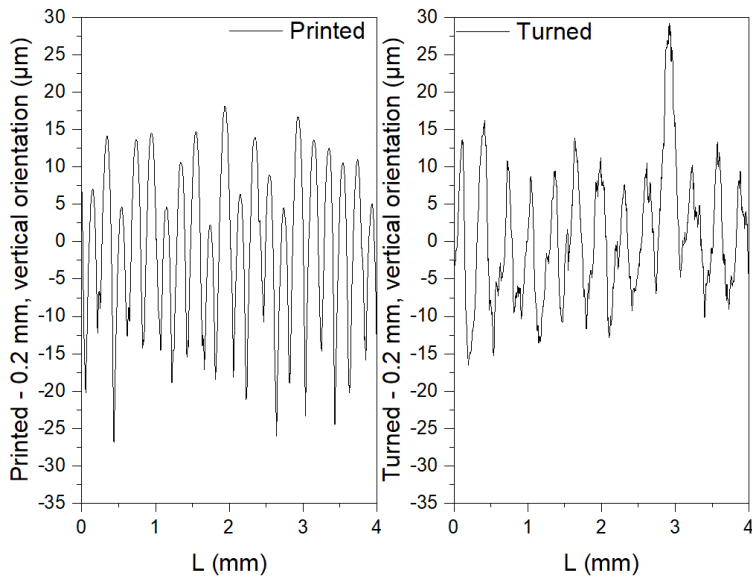


Figure 10
Roughness profiles after printing and turning

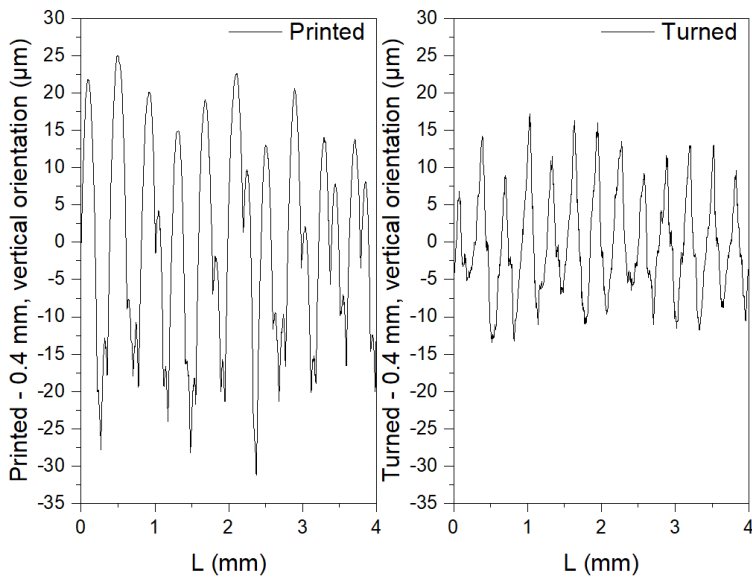


Figure 11
Roughness profiles after printing and turning

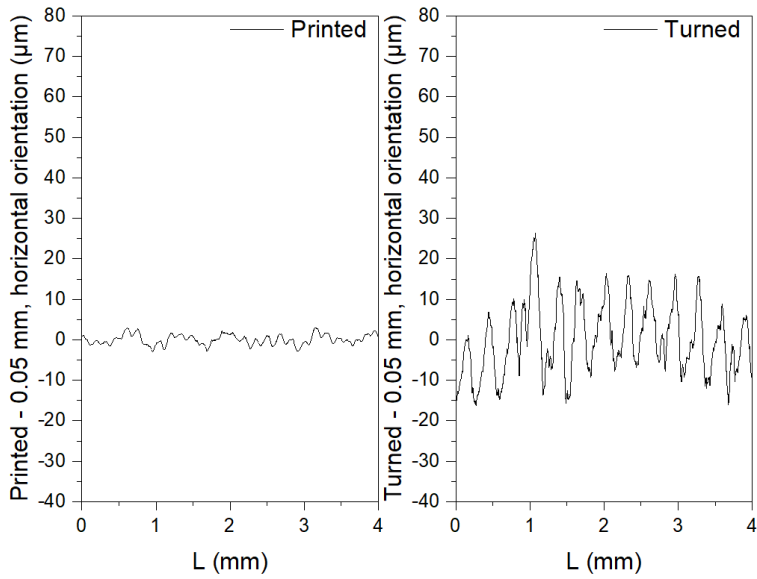


Figure 12
Roughness profiles after printing and turning

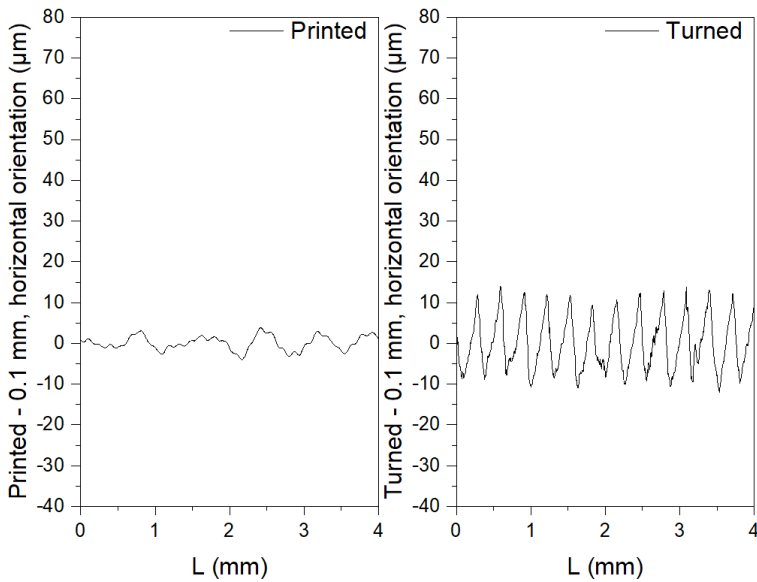


Figure 13
Roughness profiles after printing and turning

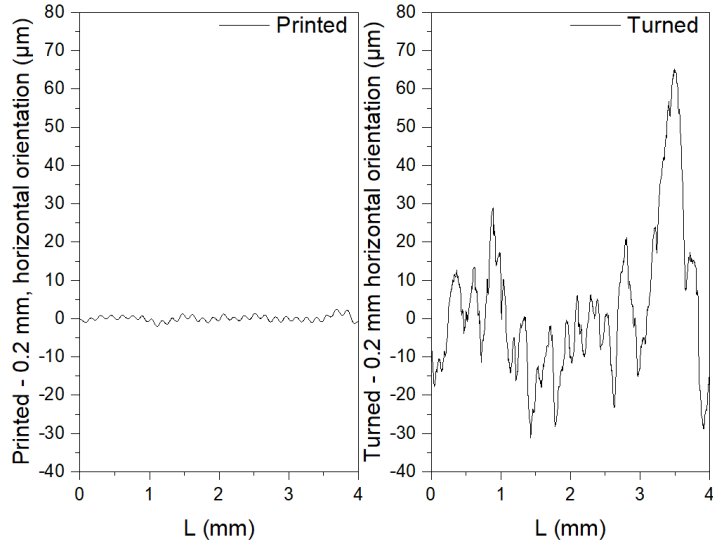


Figure 14
Roughness profiles after printing and turning

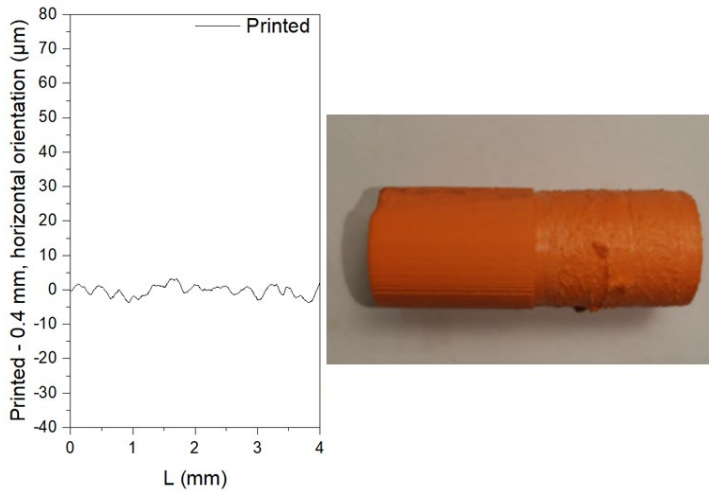


Figure 15
Roughness profiles after printing and turning

For each specimen, 3 roughness measurements were taken and then averaged, these are shown in Tables 3-6. As illustrated in Table 6 and Fig. 17, the surface roughness obtained after turning the 0.4 mm of layer thickness, horizontal oriented specimen has no data because it could not be measured as the surface was smeared during turning, as shown in Fig. 15.

Table 3

 R_a values as a function of layer thickness for vertical orientation after printing

Layer thickness	R_{a1}	R_{a2}	R_{a3}	avg. R_a	Dispersion
0.05	7.981	7.780	9.017	8.259	0.664
0.1	11.064	9.051	7.612	9.242	1.734
0.2	12.803	11.630	10.786	11.740	1.013
0.4	24.552	23.981	22.202	23.578	1.226

Table 4

 R_a values as a function of layer thickness for horizontal orientation after printing

Layer thickness	R_{a1}	R_{a2}	R_{a3}	avg. R_a	Dispersion
0.05	1.895	1.745	2.624	2.088	0.470
0.1	0.651	1.507	1.067	1.075	0.428
0.2	1.785	1.330	4.535	2.550	1.734
0.4	1.721	1.365	1.648	1.578	0.188

The average surface roughness (R_a) after printing and turning as a function of layer thickness in case of vertical orientation is shown in Fig. 16.

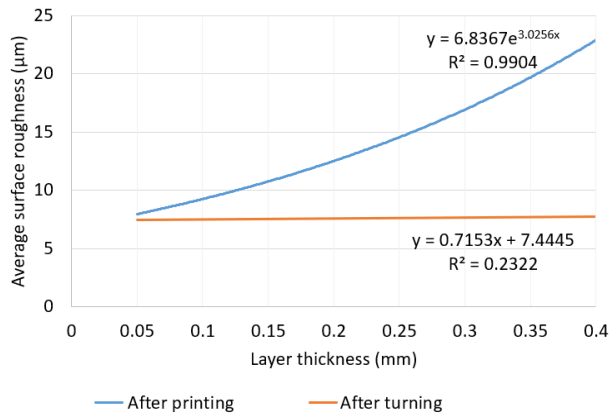


Figure 16

 R_a as a function of the layer thickness after printing and turning in case of vertical orientation

Table 5

 R_a values as a function of layer thickness for vertical orientation after turning

Layer thickness	R_{a1}	R_{a2}	R_{a3}	avg. R_a	Dispersion
0.05	7.605	7.138	6.968	7.237	0.330
0.1	8.282	7.587	7.286	7.718	0.511
0.2	7.119	7.686	8.324	7.710	0.603
0.4	7.571	8.223	7.154	7.649	0.539

Table 6
 R_a values as a function of layer thickness for horizontal orientation after turning

Layer thickness	R_{a1}	R_{a2}	R_{a3}	avg. R_a	Dispersion
0.05	8.265	7.509	8.117	7.964	0.401
0.1	6.496	6.703	6.953	6.717	0.229
0.2	12.836	13.686	11.692	12.738	1.001
0.4	n/a.	n/a.	n/a.	n/a.	n/a.

The average surface roughness after printing and turning as a function of layer thickness in case of horizontal orientation is shown in Fig. 17.

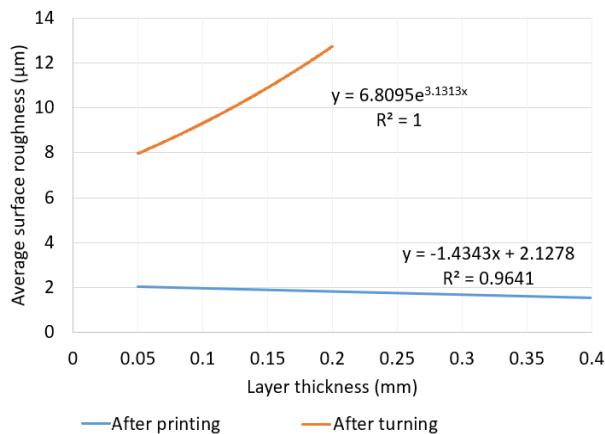


Figure 17

R_a as a function of the layer thickness after printing and turning in case of horizontal orientation

3.2 Results of Cylindricity Measurement

The deviation from nominal size and calculated tolerance as a function of layer thickness in case of vertical orientation after printing is shown in Table 7 and Fig. 18.

Table 7
 Deviation from nominal size and calculated tolerance as a function of layer thickness for vertical orientation after printing

Layer thickness	Lower limit size (mm)	Upper limit size (mm)	Tolerance field width (mm)
0.05	-0.155	0.002	0.157
0.1	-0.091	0.06	0.151
0.2	-0.035	0.111	0.146
0.4	-0.3	-0.178	0.122

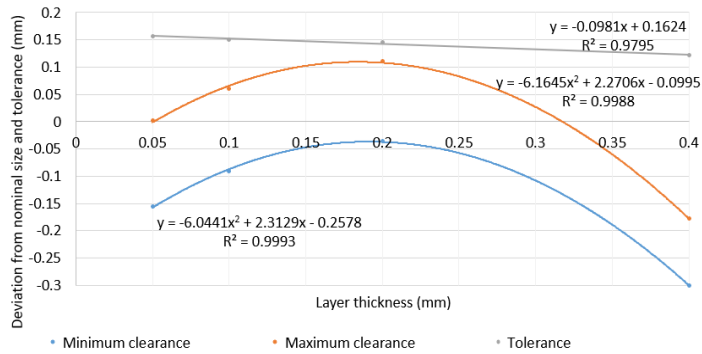


Figure 18

Deviation from nominal size and calculated tolerance as a function of layer thickness for vertical orientation after printing

The deviation from nominal size and calculated tolerance as a function of layer thickness in case of horizontal orientation after printing is shown in Table 8 and Fig. 19.

Table 8

Deviation from nominal size and calculated tolerance as a function of layer thickness for horizontal orientation after printing

Layer thickness	Lower limit size (mm)	Upper limit size (mm)	Tolerance field width (mm)
0.05	-0.097	0.296	0.393
0.1	0.012	0.352	0.34
0.2	0.095	0.36	0.265
0.4	0.343	0.688	0.345

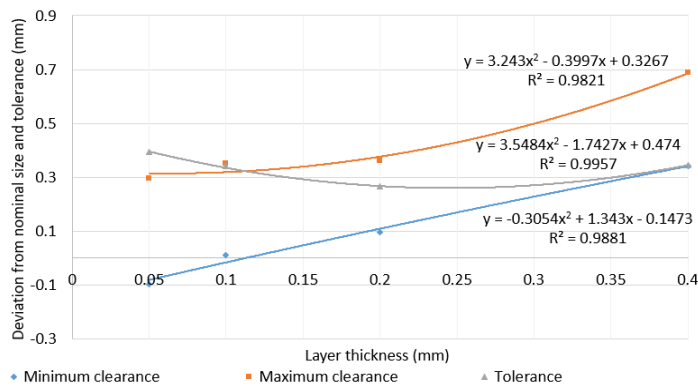


Figure 19

Deviation from nominal size and calculated tolerance as a function of layer thickness for horizontal orientation after printing

The deviation from nominal size and calculated tolerance as a function of layer thickness in case of vertical orientation after turning is shown in Table 9 and Fig. 20.

Table 9

Deviation from nominal size and calculated tolerance as a function of layer thickness for vertical orientation after turning

Layer thickness	Lower limit size (mm)	Upper limit size (mm)	Tolerance field width (mm)
0.05	-0.01	0.02	0.03
0.1	-0.01	0.03	0.04
0.2	-0.02	0.03	0.05
0.4	-0.01	0.04	0.05

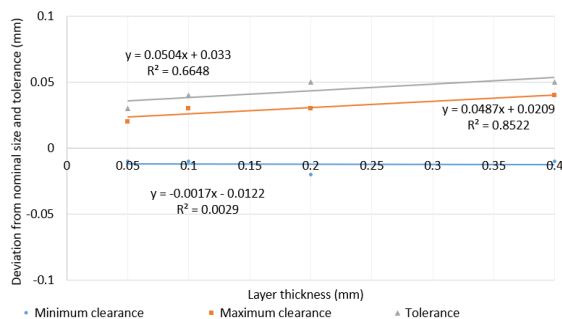


Figure 20

Deviation from nominal size and calculated tolerance as a function of layer thickness for vertical orientation after turning

The deviation from nominal size and calculated tolerance as a function of layer thickness in case of horizontal orientation after turning is shown in Table 10 and Fig. 21. As illustrated, the deviation from nominal size and calculated tolerance obtained after turning the 0.4 mm of layer thickness, horizontal oriented specimen has no data because it could not be measured as the surface was smeared during turning, as shown in Fig. 15.

Table 9

Deviation from nominal size and calculated tolerance as a function of layer thickness for horizontal orientation after turning

Layer thickness	Lower limit size (mm)	Upper limit size (mm)	Tolerance field width (mm)
0.05	-0.01	0.05	0.06
0.1	-0.03	0.04	0.07
0.2	-0.1	0.12	0.22
0.4	n/a.	n/a.	n/a.

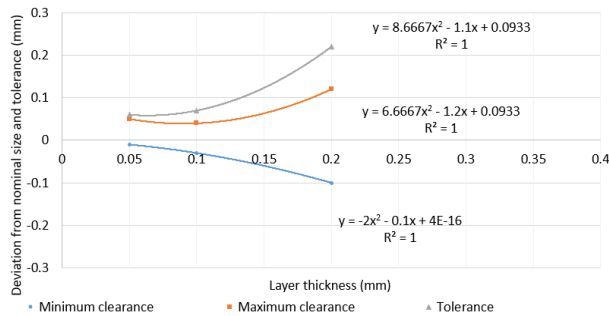


Figure 21

Deviation from nominal size and calculated tolerance as a function of layer thickness for horizontal orientation after turning

3.3 Chip Formation

The chip produced during the turning for both orientations are shown in Fig. 22.



Figure 22

Flowing chips in case of a) vertical and fragmented chips b) horizontal orientation during turning

4 Analysis

4.1 Results of the Surface Roughness Measurement

The average surface roughness values after printing and turning and their plotting are shown in Table 3., Table 5. and Fig. 16 in case of vertical orientation. The surface roughness degradation increases with increasing layer thickness in case of printed surfaces. However, this deterioration is not proportional, as it is minimal when comparing 0.05 mm and 0.1 mm layer thicknesses, but the

machining time is halved. Table 5, Fig. 8-11, and Fig. 16 show that the surface roughness measured after printing has essentially no effect on the surface roughness after turning, with values ranging from $7.2\ \mu\text{m}$ to $7.7\ \mu\text{m}$. Therefore, if the functional surface is to be produced by cutting technology, it is recommended to choose a layer thickness of 0.4 mm for printing, because it has no influence on the turned surface, but the printing time is nearly one eighth compared to the printing time required for printing with a layer thickness of 0.05 mm.

The average surface roughness values after printing and turning and their plotting are shown in Table 4, Table 6, Fig. 12-15 and Fig. 17 in case of horizontal orientation. In the case of printing, the surface roughness decreased minimally as the layer thickness increased, but this result is not significant as the measurement was taken parallel to the printing direction. However, the surface roughness increased exponentially as a function of layer thickness after turning in all cases. As shown in Fig. 15 and 17, after turning the specimen printed with a 0.4 mm layer thickness, the surface roughness could not be measured because the surface was smeared.

In the end, the results of the two orientations cannot be compared, because while in the vertical orientation the measurements were taken perpendicular to the printed layers, in the horizontal orientation the measurements were taken parallel to the layer orientation. From Fig. 16-17, it can be said that after turning, better results can be achieved in vertical orientation than in horizontal orientation, regardless of the layer thickness.

4.2 Results of Cylindricity Measurement

As illustrated in Table 7 and Fig. 18, the deviation from the nominal size increased in the negative direction with increasing layer thickness in case of vertical orientation workpieces after printing. It was also observed that as the layer thickness increased, the width of the tolerance decreased. As shown in Table 9 and Fig. 20, the layer thicknesses and the dimensional variation observed in them had no influence on the dimensional stability of the turned specimen. The target diameter of 18 mm was achieved with a tolerance of 0.03-0.05 mm due to the accuracy of the lathe.

In case of horizontal orientation, as shown in Table 8 and Fig. 19, the dimensional deviation from the nominal size increased with increasing layer thickness after printing. An optimum in dimensional stability and accuracy is observed at a layer thickness of 0.2 mm. As illustrated in Table 10 and Fig. 21, the dimensional tolerance and dimensional stability of the turned surface deteriorate with increasing layer thickness. The workpiece printed at 0.4 mm layer thickness was also not measurable because the surface was smeared during turning.

Finally, as show in Figs. 20-21, it can be determined that the accuracy and dimensional stability of the vertically printed specimen is much better than that of the horizontally printed specimens.

4.3 Chip Formation

Fig. 21 shows the resulting chips during turning. It can be observed that workpieces printed with a vertical orientation formed a flowing chip during machining, which is understandable since the direction of the printed filament is the same as the direction of the cutting speed. On the other hand, in the case of the specimens with a horizontal orientation, small, fragmented chips were formed, which is due to the direction of the printed filament being perpendicular to the direction of the cutting speed. Consequently, it is better to chip specimens in a horizontal orientation because the broken chips are easier to handle. However, chip breakage can also be improved in the vertical orientation, but further experiments are needed to investigate this.

Conclusions

As shown in Fig. 16, the roughness of the printed surface has no influence on the roughness of the turned surface, the result being almost constant as a function of the layer thickness in case of vertical orientation. Fig. 17, shows that the surface roughness of the turned surface increases as a function of layer thickness, and deteriorates to the extent that it was unmeasurable at a layer thickness of 0.4 mm. Comparing the surface roughness measured in terms of orientation, it was found that the surface roughness was better for all layer thicknesses in the vertical orientation.

Fig. 20 shows that the tolerance of the turned surfaces is nearly constant as a function of layer thickness in case of vertical orientation, so there is no effect on accuracy. On the other hand, in the horizontal orientation, the accuracy of the turned surface deteriorates significantly as a function of layer thickness, and was unmeasurable for a layer thickness of 0.4 mm. Comparing the dimensional accuracy measured in terms of orientation, it was found that it was better for all layer thicknesses in the vertical orientation.

If functional surfaces are to be finished by some cutting technology, it is advisable to choose the printing in vertical orientation with layer thickness of 0.4 mm. The surface roughness is almost constant as a function of layer thickness, and a dimensional accuracy of 0.05 is adequate for many engineering applications. Only the chip breakage is favorable for the horizontal orientation, but this can be improved by using a chip breaker or by modifying the process parameters. The latter, will require further investigation.

References

- [1] P. Ficzere, "The Impact of the Positioning of Parts on the Variable Production Costs in the Case of Additive Manufacturing," *Periodica Polytechnica Transportation Engineering*, Vol. 50, No. 3, pp. 304-308, 2022
- [2] P. Ficzere et al., "ECONOMICAL INVESTIGATION OF RAPID PROTOTYPING," *INTERNATIONAL JOURNAL FOR TRAFFIC AND TRANSPORT ENGINEERING*, Vol. 3, No. 3, pp. 344-350, 2013
- [3] A. Takacs, "Safe In and Out of the Car," In: *Jármai, K., Cservenák, Á. (eds) Vehicle and Automotive Engineering 4. VAE 2022. Lecture Notes in Mechanical Engineering*, Miskolc, Hungary, pp. 63-70, 2023
- [4] B. Ádám, Z. Weltsch, "Thermal and Mechanical Assessment of PLA-SEBS and PLA-SEBS-CNT Biopolymer Blends for 3D Printing," *Applied Sciences* 2021, Vol. 11, No. 13, p. 6218, 2021
- [5] R. Velu et al., "3D printing technologies and composite materials for structural applications," *Green Composites for Automotive Applications*, pp. 171-196, 2019
- [6] C. W. J. Lim et al., "An Overview of 3-D Printing in Manufacturing, Aerospace, and Automotive Industries," *IEEE Potentials*, Vol. 35, No. 4, pp. 18-22, 2016
- [7] K. Tomasz et al., "Emission of particles and VOCs at 3D printing in automotive," *Smart Innovation, Systems and Technologies*, Vol. 155, pp. 485-494, 2019
- [8] F. Garai et al., "Development of tubes filled with aluminium foams for lightweight vehicle manufacturing," *Materials Science and Engineering A*, Vol. 790, 2020
- [9] S. M. M. Hanon et al., "Tribological Behaviour Comparison of ABS Polymer Manufactured Using Turning and 3D Printing," *International Journal of Engineering and Management Sciences*, Vol. 4, No. 1, pp. 46-57, 2019
- [10] B. Ádám et al., "THE EFFECT OF DIFFERENT PRINTING PARAMETERS ON MECHANICAL AND THERMAL PROPERTIES OF PLA SPECIMENS," *Gradus*, Vol. 7, No. 3, pp. 166-173, 2020
- [11] K. Kun, "Reconstruction and development of a 3D printer using FDM technology," *Procedia Engineering*, Vol. 149, pp. 203-211, 2016
- [12] K. Kandanond, "Surface Roughness Reduction in A Fused Filament Fabrication (FFF) Process using Central Composite Design Method," *Production Engineering Archives*, Vol. 28, No. 2, pp. 157-163, 2022

- [13] A. W. Hashmi et al., “The Surface Quality Improvement Methods for FDM Printed Parts: A Review,” *Fused Deposition Modeling Based 3D Printing*, pp. 167-194, 2021
- [14] B. Gadagi and R. Lekurwale, “A review on advances in 3D metal printing,” *Materials Today: Proceedings*, Vol. 45, pp. 277-283, 2021
- [15] S. R. S. Bharathi et al., “Multi objective optimization of CNC turning process parameters with Acrylonitrile Butadiene Styrene material,” *Materials Today: Proceedings*, Vol. 27, pp. 2042-2047, 2020
- [16] M. Trifunović et al., “Investigation of cutting and specific cutting energy in turning of POM-C using a PCD tool: Analysis and some optimization aspects,” *Journal of Cleaner Production*, Vol. 303, p. 127043, 2021
- [17] I. Fekete et al., “Highly toughened blends of poly(lactic acid) (PLA) and natural rubber (NR) for FDM-based 3D printing applications: The effect of composition and infill pattern,” *Polymer Testing*, Vol. 99, p. 107205, 2021
- [18] T. Yao et al., “A method to predict the ultimate tensile strength of 3D printing polylactic acid (PLA) materials with different printing orientations,” *Composites Part B: Engineering*, Vol. 163, pp. 393-402, 2019
- [19] A. Nugroho et al., “Effect of layer thickness on flexural properties of PLA (PolyLactid Acid) by 3D printing,” *Journal of Physics: Conference Series*, Vol. 1130, No. 1, p. 012017, 2018
- [20] A. Piros L. Trautmann, “Creating interior support structures with Lightweight Voronoi Scaffold,” *International Journal on Interactive Design and Manufacturing*, Vol. 17, No. 1, pp. 93-101, 2023
- [21] G. K. Maharjan et al., “Compressive Behaviour of 3D Printed Polymeric Gyroid Cellular Lattice Structure,” *IOP Conference Series: Materials Science and Engineering*, Vol. 455, No. 1, p. 012047, 2018
- [22] Sulinet knowledge base, “Tolerances and fits”, [online] Available at: <https://tudasbazis.sulinet.hu/hu/szakkepzes/mezogazdasag/muszaki-alapismeretek/alakturesek/alakturesek> [Accessed: 14. 02. 2023.]